TanDEM-X Experiments in Pursuit Monostatic Configuration

Pau Prats, Rolf Scheiber, Josef Mittermayer, Steffen Wollstadt, Stefan V. Baumgartner, Paco López-Dekker, Daniel Schulze, Ulrich Steinbrecher, Marc Rodríguez-Cassolà, Andreas Reigber, Gerhard Krieger, Manfred Zink, Alberto Moreira

German Aerospace Center (DLR), Microwaves and Radar Institute, Germany

Abstract

This paper reports on several experiments performed by the TanDEM-X constellation that could be potentially implemented as operational modes in future SAR missions. Many of them have been already demonstrated experimentally and could be repeated during a possible next pursuit monostatic phase with TanDEM-X. The new modes include new single-look products as well as interferometric ones, some of which are included in this paper as an example of their potential performance.

1 Introduction

The TanDEM-X constellation [1] has proven to be the perfect test-bed for future SAR missions. Several experiments have been performed since the launch of the TanDEM-X (TDX) satellite on June 21st, 2010, including both single-look products and new interferometric modes. Due to their application potential, some of them could be implemented as operational modes in future SAR missions. The next section briefly explains each of these experiments, highlighting their potentials and benefits.

2 Single-Look Products

2.1 Improved Resolution

The operational products of TerraSAR-X (TSX) and TDX satellites offer a minimum resolution of about 1 x 1 meter in the high-resolution spotlight mode with a scene extension of 5 x 5 km. In [2] it was suggested to use both satellites to improve the resolution of the imaging products by combining coherently the TSX and TDX spectra. This was done in range and azimuth independently, but the improvement might be done simultaneously for both by doubling the PRF. **Figure 1** (top) shows an example of a range-resolution-enhanced product over Sydney, Australia, with a final range resolution of 300 MHz by combining two images with 150 MHz bandwidth each. Figure 1 (bottom) shows an azimuth-resolution-enhanced example over Neustrelitz, Germany, with a final azimuth resolution of 1.5 m after combining the adjacent Doppler spectra of TSX and TDX. The measurement over a corner reflector (CR) in this later scene confirms the resolution improvement, as shown in **Figure 2**.

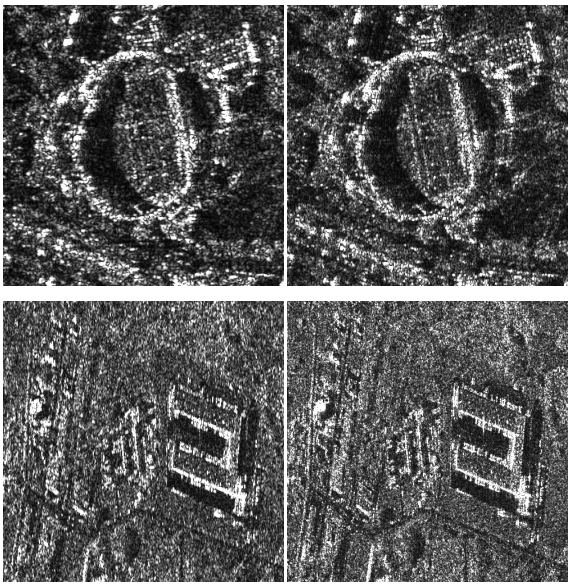

Figure 1 Demonstration of distributed imaging with TSX and TDX. (Left column) Single channel images, and resolution-improved products in (top right) range and (bottom right) azimuth. Range is horizontal and azimuth is vertical.

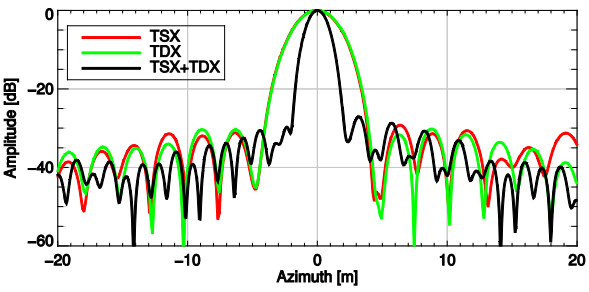

Figure 2 Azimuth profile of the impulse response function of a CR showing the resolution improvement after combining the two azimuth spectra.

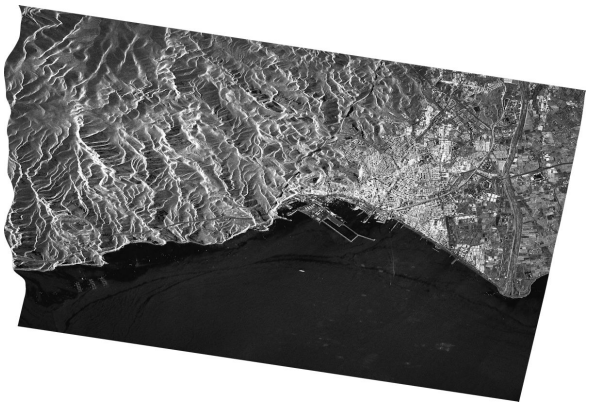

Figure 3 Geocoded sliding spotlight image over Almería, Spain, with a nominal 0.8m azimuth resolution and 10 km azimuth scene extension.

A bistatic spotlight product could use larger steering angles (max ± 2.2º) in order to increase the azimuth observation times. Such large angles would produce grating lobes in the synthesized antenna pattern, but a bistatic operation combined with a sufficiently large along track distance (e.g. 20 km) would not be influenced by them in terms of azimuth ambiguities. Such a mode could potentially obtain azimuth resolutions below 0.5 m and a scene extension in the order of 3 – 4 km with a staring spotlight operation, or resolutions of 1 m and a scene extension of 10 km with sliding-spotlight. Note that due to the large along-track separation and observation times, a dedicated bistatic processing kernel would need to be selected.

Figure 3 shows a monostatic sliding-spotlight image over Almería, Spain, with an azimuth extension of 10 km and a nominal azimuth resolution of 0.8 m. Due to the monostatic operation, the grating lobes introduce higher azimuth ambiguities, some of which are noticeable over the sea area. Note that the sliding spotlight (SL) operational product has an azimuth extension of 10 km with only 1.7 m azimuth resolution, while the numbers for the high resolution spotlight (HS) operational product are 5 km and 1 m, respectively.

2.2 Bi-Directional SAR

The bidirectional SAR (BiDi SAR) mode has been

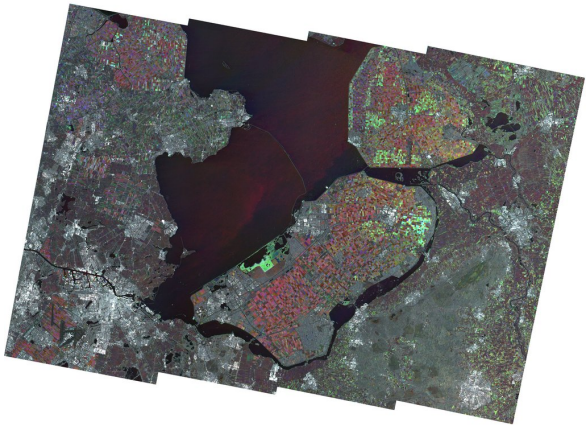

Figure 5 RGB composite of three different TOPS data takes over Flevoland, The Netherlands, acquired by TerraSAR-X. The dates are 01.04.2010, 15.05.2010, 17.06.2010, corresponding to the vegetation growth period.

recently demonstrated with TSX [3]. In this mode, the azimuth antenna pattern is configured to have two beams of equal power with a separation of about 4º, i.e. the main beam and the grating lobe have the same magnitude. Such a configuration allows the simultaneous acquisition of the same scene with two different squint angles, which inherently implies a certain temporal separation (about 6 seconds between the fore and aft images in the TSX case). **Figure 4** shows an example of a BiDiSAR acquisition over Singapore. Many applications could benefit of the potentials such a mode offers, e.g. traffic monitoring.

2.3 Quad-Pol Synthesis using Dual-Pol Data

Also in [2] the simulation of quad-pol images by combining interferometric dual-pol data acquired by TSX and TDX independently was suggested. Similar as in 2.1.1, the SLCs need to be processed coherently in order to remove the baseline information and generate the quad-pol product. TerraSAR-X offers quad-pol products only experimentally, and with the limitation inherent to the dual receive antenna (DRA) mode. This reduces the performance in terms of azi-

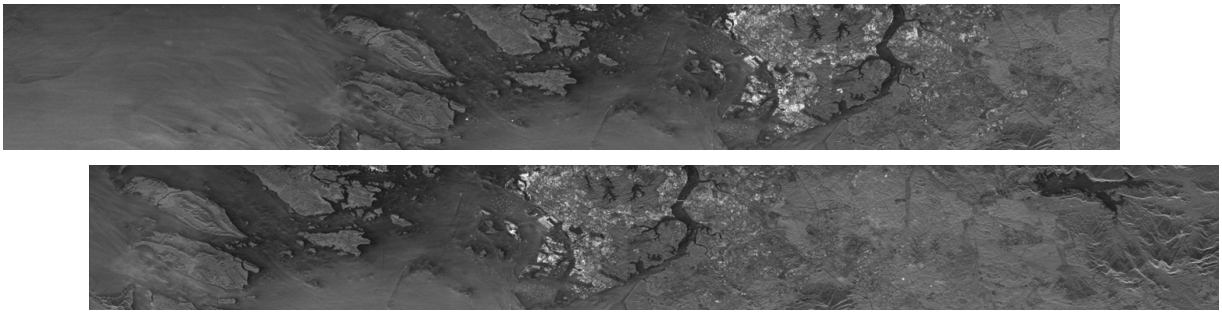

Figure 4 TSX images acquired over Singapore in one pass with the BiDiSAR mode: (top) Backward and (bottom) forward images.

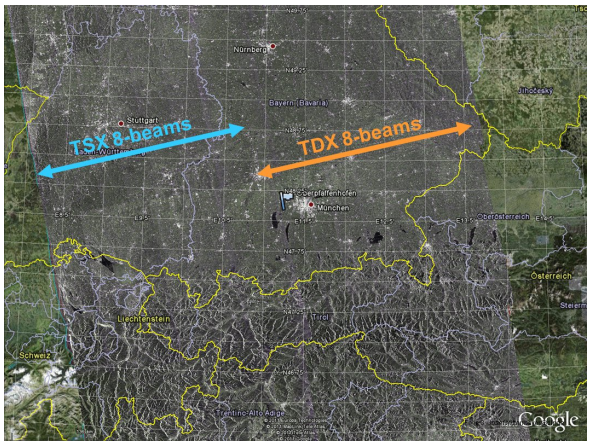

Figure 6 Example of two 8-beam ScanSAR acquisitions over Germany acquired simultaneously by TSX and TDX during the pursuit monostatic commissioning phase. The coverage is 200 km for each acquisition, making a total of 400 km.

muth ambiguities and SNR. A quad-pol synthesis approach would not have such drawbacks, hence offering a quality product comparable to the operational ones offered by TSX.

2.4 TOPS

The TOPS mode was first demonstrated in-orbit by TSX [4], and will be the default mode of ESA's Sentinel-1 satellite. This new wide-swath imaging mode circumvents the limitations of ScanSAR, namely an azimuth-varying DTAR and SNR, by steering the antenna from backwards to forward during the acquisition of the burst. Thanks to this steering, all targets within a burst are observed by the same antenna pattern, hence avoiding an azimuth-varying sensitivity. **Figure 5** shows a RGB composite of three different data takes over Flevloand, the Netherlands, acquired at different dates by TSX. Note the absence of scalloping in the amplitude.

2.5 Ultra-Wide Swath Modes

The trade-off between resolution and coverage in the wide-swath modes (TOPS and ScanSAR) could be further exploited with TSX and TDX. As a result, it is possible to obtain products with up to 8 sub-swaths with an azimuth resolution of about 40 m, resulting in a swath coverage of 200 km. By combining both satellites flying in the pursuit monostatic formation, a total swath of 400 km can be covered. This is exemplified in **Figure 6** with two 8-beam ScanSAR images acquired over Germany. The images were acquired at the same time by TSX and TDX during the pursuit monostatic commissioning phase of the TanDEM-X mission.

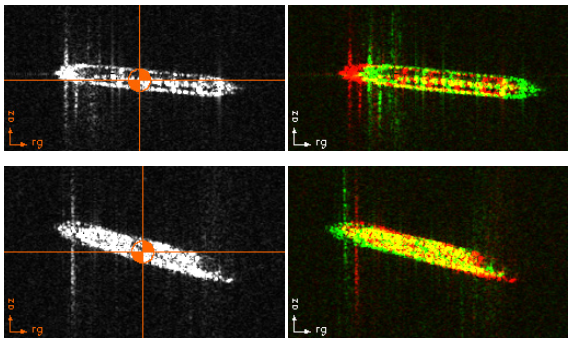

Figure 8 TSX images of two vessels (left col; the orange crosses mark the points used for georeferencing) and corresponding superpositions with TanDEM-X images (right col; TerraSAR-X image in red, TanDEM-X image in green).

3 Interferometric Products

The TanDEM-X constellation offers a unique opportunity to acquire interferometric data with varying baselines, both in time and space. The main mission objective already exploits the single-pass capabilities in order to produce a global DEM with unprecedented accuracy [1]. In a possible next pursuit monostatic phase, different time and space baselines could be possible, hence offering new opportunities for further applications. The baseline in time is probably the more appealing one, since many applications would benefit from it, including sea currents, traffic monitoring, or glaciers.

3.1 Traffic Monitoring

A first clear example is the use of the temporal baseline for traffic monitoring. Such capabilities were already demonstrated during the first pursuit monostatic phase [5]. **Figure 8** shows a result of these experiments, where the two satellites observed the same area with just three seconds difference, enough to measure the velocity vector of several ships navigating through the Strait of Gibraltar. Also in [5], GMTI techniques with TSX and TDX were demonstrated over land traffic.

3.2 New Interferometric Modes

Some of the modes mentioned in Section 2.1 would increase its potential when exploited interferometrically, e.g. wide-swath interferograms. As an example, **Figure 9** shows the subsidence measured over Mexico City with differential SAR interferometry using two TOPS images acquired with 4 months separation.

The combination of interferometry with the bi-directional SAR mode offers also many interesting possibilities, including a larger sensitivity to the measurement of the along-track shift between images

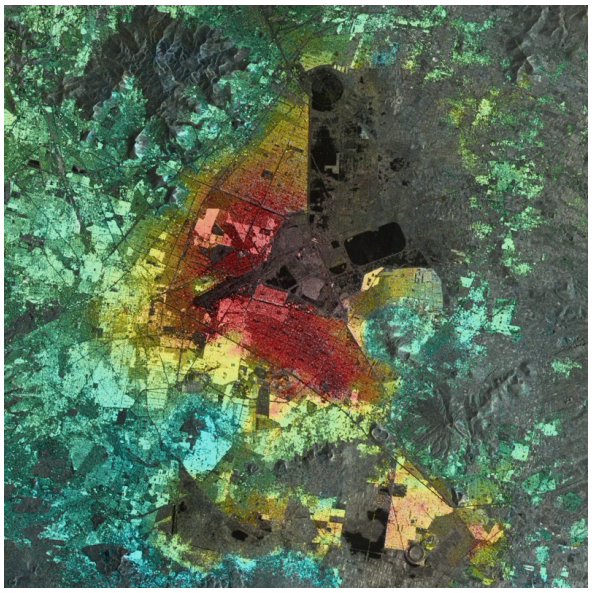

Figure 9 Geocoded deformation measured with differential SAR interferometry over Mexico City using 2 TOPS images separated 4 months. The deformation goes from -10 cm (red) to +10 cm (dark blue).

[6]. The flexibility in the selection of the time baseline implies that a wide range of applications could benefit from such potential.

A further example of the potential of a pursuit monostatic configuration is the monitoring of sea ice dynamics with along-track interferometry [7]. The top plot of **Figure 10** shows an along-track interferogram obtained in scanSAR mode near the east coast of Greenland. The interferogram reveals cyclic fringe patterns of the individual ice blocks, which are due to rotation about their vertical axes. From these patterns, the rotation can be derived with high accuracy, as shown in the lower plot of Figure 10. Again, the separation between acquisitions was about three seconds.

4 Summary

This contribution has showed the potential of new modes and products for future satellite constellations. Several possibilities have been listed and some of them have already been demonstrated during the pursuit monostatic commissioning phase of the TanDEM-X mission.

References

[1] G. Krieger *et al*, "TanDEM-X: A satellite formation for high-resolution SAR interferometry," *IEEE Trans. on Goesci. and Remote Sening*, 45, 11, pp. 3317–3341, Nov. 2007.

[2] P. Prats *et al*, "Distributed Imaging with TerraSAR-X and TanDEM-X," *Proc. IGARSS*, Vancouver, Canada, 2011.

[3] J. Mittermayer *et al.*, "Simultaneous Bidirectional SAR Acquisition with TerraSAR-X," *Proc. EUSAR*, Aachen, Germany, 2010.

[4] A. Meta *et al.*, "TOPS Imaging with TerraSAR-X: Mode Design and Performance Analysis," *IEEE Trans. on Goesci. and Remote Sening*, 48, 2, Feb. 2010.

[5] S. Baumgarter *et al.*, "Large Along-Track Baseline SAR-GMTI: First Results with the TerraSAR-X/TanDEM-X Satellite Constellation," *Proc. IGARSS*, Vancouver, Canada, 2011.

[6] J. Mittermayer *et al.*, "Bi-directional SAR and Interferometric SAR Short Term Time Series," *Proc. EUSAR*, Nürnberg, Germany, 2012.

[7] R. Scheiber *et al.*, "Interferometric Sea Ice Mapping with TanDEM-X: First Experiments," *Proc. IGARSS*, Vancouver, Canada, 2011.

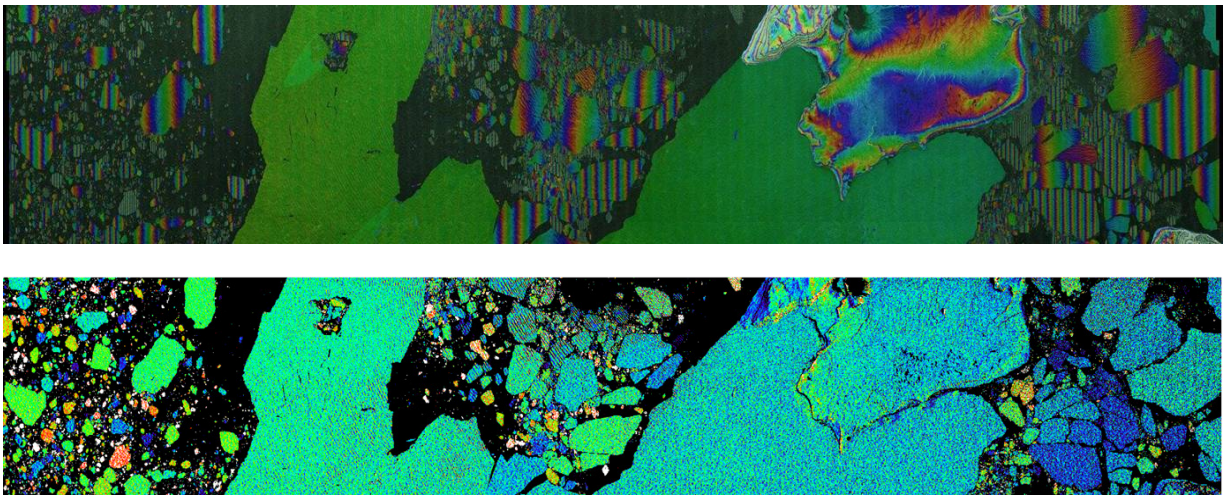

Figure 10 Coastal area in North-East Greenland observed on 2nd August, 2010 by TerraSAR-X and TanDEM-X. (top) Interferometric phase for the three second interval of the data acquisition, (bottom) sea-ice rotation map scaled from -0.005 (yellow to red) to +0.005 deg (blue to violet). The rotation has been derived from the frequency of the vertical fringes observed on the top figure.